Journal of Materials Chemistry

Cite this: J. Mater. Chem., 2011, 21, 14807

www.rsc.org/materials

PAPER

Chiral liquid crystalline compounds with a re-entrant SmA* phase†

Vladimíra Novotná,*[a] Věra Hamplová,[a] Natalia Podoliak,[a] Miroslav Kašpar,[a] Milada Glogarová,[a] Damian Pociecha[b] and Ewa Gorecka[b]

Received 13th May 2011, Accepted 1st July 2011
DOI: 10.1039/c1jm12131f

Unusual mesomorphic behaviour has been found in a series of rod-like liquid crystalline (LC) compounds with two chiral centres in the molecular chain. A re-entrant paraelectric SmA* (SmA^*_{RE}) phase has been discovered below the ferroelectric SmC* phase on cooling for one homologue. So far this compound is the only one exhibiting the re-entrancy of the smectic A phase in chiral LC system with structural parameters so close to the upper SmA* phase. X-Ray studies, as well as dielectric spectroscopy, spontaneous polarization and tilt angle measurements have been carried out to characterize studied compounds. We compare various homologues and look for tendencies in physical properties behaviour.

Introduction

Liquid crystalline (LC) materials exhibit a rich variety of phases. One can predict stability of different phases on a scale of decreasing temperature taking into account that a decrease of temperature leads to an increase of molecular order. Re-entrancy means that a less ordered system appears on cooling below a more ordered one. This phenomenon can be observed in liquid crystals[1] due to a large number of competing interactions (*e.g.* competing order parameters and their fluctuations[1a]) and temperature dependent molecular conformations. In spite of the fact that re-entrancy has been observed several times in LC systems,[2] origin of this effect has not been completely understood and unsolved problems connected with re-entrancy still exist in condensed state physics.

Compounds with chiral rod-like molecules exhibit LC phases with structures related to those of non-chiral moieties, but with different properties. Smectic phases with molecules tilted towards layer normal show ferroelectricity, spontaneous polarization and piezoelectric properties. Nowadays, lactic acid unit is frequently used as a basis of a chiral part of rod-like molecules and these liquid crystalline compounds show a variety of liquid crystalline phases in a broad temperature range.[3]

Herein, we are reporting a new series of chiral liquid crystalline compounds based on a molecular core formed by two biphenyls connected by an ester linkage group with two chiral centres in the terminal part. Recently it has been discovered that one homologue exhibits re-entrancy of a smectic A phase below the ferroelectric SmC* phase.[4] We assigned this phase to re-entrant smectic A phase (SmA^*_{RE}) and it is the first example of smectic A phase re-entrancy in a chiral smectic system. The SmA^*_{RE} phase shows the same structural parameters as the upper SmA* phase so we can exclude formation of dimers or intercalated layers. The SmA^*_{RE} phase has been described on the basis of mean field theory[4] taking into account non-monotonous temperature dependence of the lowest term coefficient in thermal expansion. In this contribution we are presenting synthesis and physical properties of all homologues from this unique series. We compare various homologues and look for tendencies in behaviour of physical properties when changing the length of the non-chiral chain.

Experimental

Materials

We have synthesized a new homologue series of chiral rod-like molecules consisting of two biphenyls connected by an ester group, one biphenyl being laterally substituted by a chlorine atom. The chiral part contains two chiral centres: methyl-butyl and a lactate group. General formula of the studied materials denoted as **nZBL** is in Scheme 1. Synthesis of studied compounds was carried out according to the synthesis path described in Scheme 2. The synthesis procedure and NMR results are

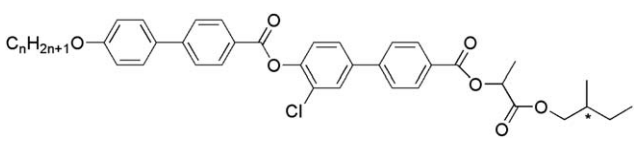

Scheme 1 Chemical formula for the homologues series **nZBL**.

[a]*Institute of Physics, Academy of Science of the Czech Republic, Na Slovance 2, CZ-182 21 Prague 8, Czech Republic. E-mail: novotna@fzu.cz; Fax: +420286890527; Tel: +420266053111*
[b]*Laboratory of Dielectrics and Magnetics, Chemistry Department, Warsaw University, Al. Zwirki i Wigury 101, 02-089 Warsaw, Poland. E-mail: pociu@chem.uw.edu.pl; Fax: +48228221075; Tel: +48228221075*
† Electronic supplementary information (ESI) available. See DOI: 10.1039/c1jm12131f

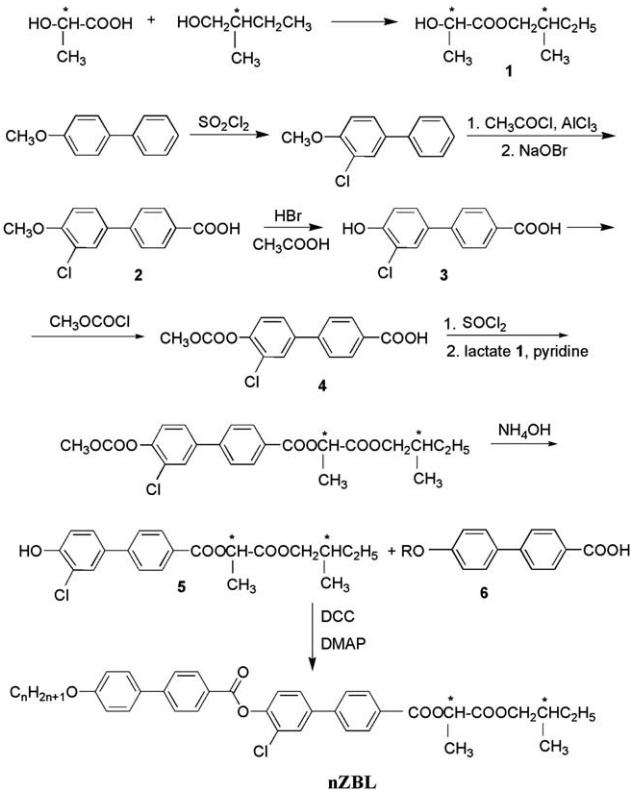

Scheme 2 Synthesis route for **nZBL** series preparation.

presented in ESI.† Both chiral centres have (*S*) configuration. We have varied a number of carbon atoms in the non-chiral chain (*n*). Molecular structure of all synthesized compounds was checked using standard analytical methods. ^{1}H NMR spectra were acquired on spectrometer Varian-Gemini 300 HC, deuterochloroform and DMSO-d_6 serving as the solvents and the signals of the solvents were used as internal standards. Chemical shifts are given in δ-scale (ppm), coupling constant J(H,H) in Hz. IR spectra were recorded on Nicolet FTIR 740 spectrometer in chloroform. Column chromatography was carried out under atmospheric pressure using silica gel (100–200 mesh, Merck).

Physical studies

Phase transition temperatures and enthalpies were determined by DSC studies (Pyris Diamond Perkin-Elmer 7) during cooling and heating runs at a rate of 5 K min^{-1}. Samples of 2–5 mg were hermetically sealed in aluminium pans and placed in the calorimeter chamber inflated by nitrogen. Texture observation and studies of other physical properties were carried out on planar samples filled by capillary action in the isotropic phase into cells composed of glasses with ITO transparent electrodes (5 × 5 mm^2). Commercial cells with homogeneous alignment (planar geometry) were used with a thickness of about 8 μm. Besides, home-made cells of 12 μm were prepared without any surfactant or surface treatment and with mylar folia as spacers.

Frequency dispersion of permittivity was measured on cooling using Schlumberger 1260 impedance analyzer in a frequency range of 1 Hz–1 MHz, keeping the temperature of the sample stable during frequency sweeps within ±0.1 K. The frequency dispersion data were analyzed using the Cole-Cole formula for the frequency dependent complex permittivity complemented by the second and the third terms to eliminate the low frequency contribution from D.C. conductivity σ and the high frequency contribution due to resistance of the ITO electrodes, respectively:

$$\varepsilon^* - \varepsilon_\infty = \frac{\Delta\varepsilon}{1 + (if/f_r)^{(1-\alpha)}} - i\left(\frac{\sigma}{2\pi\varepsilon_0 f^n} + Af^m\right), \qquad (1)$$

where f_r is the relaxation frequency, $\Delta\varepsilon$ the dielectric strength, α the distribution parameter of relaxation, ε_0 the permittivity of vacuum, ε_∞ the high frequency permittivity and n, m, A are parameters of fitting. Measured real, ε', and imaginary, ε'', parts of dielectric permittivity $\varepsilon^*(f) = \varepsilon' - i\varepsilon''$ were simultaneously fitted to formula (1).

Small angle X-ray diffraction studies were performed using Bruker D8 Discover system (Cu-Kα radiation) equipped with Anton Paar DCS-350 heating stage (temperature stability 0.1 K), working in the reflection mode. Samples were prepared as one-surface-free droplets on a heated surface. X-Ray studies were checked using the Bruker Nanostar system (Cu-Kα radiation, Vantec 2000 area detector, MRI TCPU H heating stage) working in the transmission mode. The temperature stability was 0.1 K. Powder samples for Nanostar were prepared in thin-walled glass capillaries (1.5 mm diameter).

Tilt angle was measured by a method of rotating analyzer, described in detail in the literature.[5] He–Ne laser beam was circularly polarized by a Glan-Thompson prism and a quarter-wave plate. Switching voltage with a rectangular profile at 120 Hz was applied to a sample. After passing through the rotating analyzer (strong synchronous motor was used at frequency 90 Hz) the light was detected by a photodiode and fed to the input of the oscilloscope. The intensity data waveform was decomposed into two sinusoidal curves and numerically analyzed to obtain a phase difference.

Measurements of the spontaneous polarization were carried out by integrating polarization reversal current under a triangular field. The hysteresis loop profile was checked by a Tektronix TDC70 oscilloscope using a modified Sawyer-Tower bridge method.

Results

Mesomorphic properties

All compounds exhibit the Ch-TGBA-SmA* phase sequence, and for materials with n higher than 7 a blue phase (BP) appears on cooling from the isotropic one. Both the BP and TGBA (twist grain boundary) phases exist in a very narrow temperature interval contrary to the SmA* phase existing in an interval up to 120 degrees for **8ZBL**. For compounds with n = 9 and 10 the SmC* phase occurs. For **9ZBL** another smectic phase has been discovered below the SmC* one on cooling. This phase was attributed to a re-entrant smectic A phase, the phase transition SmC*-SmA*$_{RE}$ has been theoretically described in ref. 4. A typical DSC plot is presented in Fig. 1 for **9ZBL** exhibiting the richest polymorphism. The high temperature part is shown in enlarged view in the inset. One can see that crystallization and melting peaks are sharp (for **9ZBL** see Fig. 1) and all phase transition temperatures lie above the melting point, which

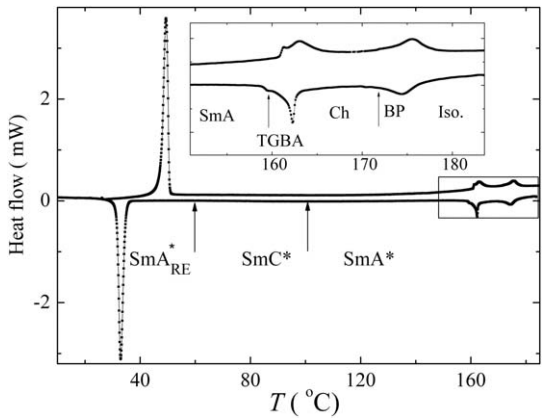

Fig. 1 DSC plot for **9ZBL**. The upper and lower curve shows the second heating and subsequent cooling run, respectively, at a rate of 5 K min^{-1}. In the inset, a vicinity of the Iso-BP-Ch-TGBA-SmA* phase transitions is enlarged. Arrows mark the SmA*-SmC* and SmC*-SmA*$_{RE}$ phase transitions not recognizable by DSC measurements (temperatures taken from other experimental techniques).

evidences enantiotropic character of the observed phases. In the Fig. 2 phase diagram for the whole homologue series **nZBL** is presented. Table 1 summarizes phases, phase transition temperatures and corresponding enthalpies obtained from DSC measurements. The SmA*-SmC*-SmA*$_{RE}$ phase transitions are not recognizable in calorimetric measurements, the transition temperatures are taken from a microscope observation or from other experimental techniques.

Texture studies and optical properties

Planar samples (bookshelf geometry) 8 μm thick were studied under a polarizing microscope. Observed blue phase texture exhibits plate- like domains characteristic for a blue phase (BP).[6] In the cholesteric phase an oily-streak texture was found. In the TGBA phase typical coloured blurry pseudo-fan texture was observed.[7] On cooling, the TGBA-SmA* phase transition was manifested as an abrupt sharpening of contrast and a change of fan colour. Colour of fan-shaped texture gradually changed on cooling continuously through the SmA* and SmC* phases showing an increase of birefringence. No dechiralization lines or

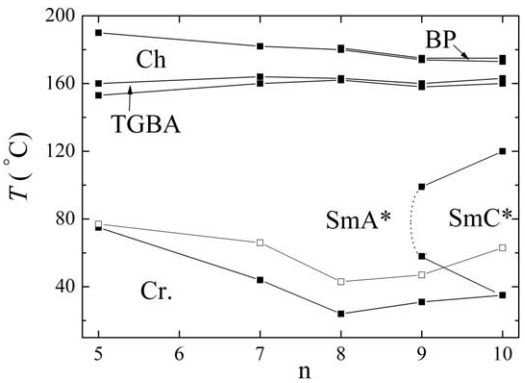

Fig. 2 Phase diagram for **nZBL** compounds. Empty symbols show melting points.

other textural features or defects appeared in the SmC* phase of ferroelectric compounds **9ZBL** and **10ZBL**. For **9ZBL** there is a moderate change in colour and slight textural modification at the transition to the SmA*$_{RE}$ phase. In the SmA*$_{RE}$ a fan-shaped texture occurs typical for non-tilted (orthogonal) smectic phase with no in-plane order. Microphotographs of textures are presented in ESI.†

Free-standing films with smectic layers parallel to the sample plane have been prepared and observed under polarizing microscope. In the TGBA phase a typical filament texture has been found. Both SmA* and SmA*$_{RE}$ phases appeared black in crossed polarizers, which confirmed an orthogonal structure. In the SmC* phase a schlieren texture has been observed with characteristic point defects. Its low contrast suggested a low tilt of molecules. By a selective reflection the helicity of both compounds **9ZBL** and **10ZBL** was established with a short helix pitch below 0.1μm.

Layer spacing

Small angle X-ray diffraction (SAXRD) studies have been performed on cooling from the isotropic phase and the layer spacing, d, has been evaluated from the peak of diffracted intensity. Temperature dependencies of d shown in Fig. 3 exhibit a gradual increase of d in the SmA* phase for all studied compounds. For **9ZBL** and **10ZBL** a decrease of d has been observed at the SmA*-SmC* phase transition, connected definitely with the tilt of molecules. Nevertheless, a tendency of d to increase on cooling dominates within the SmC* phase and thus d again increases after reaching a minimum. For **9ZBL** maximum drop down is less than 0.5% when we compare with the d value at the SmA*-SmC* phase transition and 1% if we extrapolated d linearly. For **9ZBL** the temperature evolution of d taken on cooling is presented simultaneously with the corresponding intensity of X-ray scattering peak in Fig. 4. Two phase transitions are distinguished at temperatures $T = 92$ °C and $T = 58$ °C on temperature dependencies of layer spacing as well as the diffracted intensity. They correspond to the SmA*-SmC* and SmC*- SmA*$_{RE}$ transitions observed in the texture study. The minima of diffracted intensity at the transitions reflect fluctuations.

For **9ZBL** X-ray measurement was performed subsequently during the cooling and heating runs. Both anomalies mentioned above are observed on cooling as well as on heating with a temperature hysteresis lower than 1 K. The wide angle X-ray diffraction did not detect any order in the smectic layers, so that hexatic or crystalline order is excluded even in the phase below 58 °C which was denoted as SmA*$_{RE}$. Moreover, the d values found in the SmA*$_{RE}$ phase exclude formation of smectic bilayers that occurs in some compounds with the re-entrant A phase below the nematic phase.[1] The thermal expansion coefficient taken from linear extrapolation of $d(T)$ is −0.018 Å/deg in the upper SmA* phase and −0.023 Å/deg in the SmA*$_{RE}$ phase.

Dielectric spectroscopy

Dielectric spectroscopy has been performed for **9ZBL** and **10ZBL** with the aim to establish polar fluctuations. One distinct mode has been detected in studied smectic phases and fitted using the modified Cole-Cole formula (1). Temperature dependencies

Table 1 Melting point, Mp, phase transition temperatures, T_{tr}, and temperature of crystallization, T_{cr}, in °C and corresponding enthalpies, ΔH in kJ mol^{-1}, detected on the second temperature run at a rate of 5 K min^{-1}. Star indicates the phase transition not recognisable in the DSC plots, determined from texture observation for the blue phase, and for other phases also by dielectric spectroscopy and X-ray temperature dependencies. Designation of compounds **nZBL** corresponds to Scheme 1

	Mp [ΔH]	T_{cr} [ΔH]	SmA_{RE}	T_{tr}	SmC*	T_{tr} [ΔH]	SmA	T_{tr} [ΔH]	TGBA	T_{tr} [ΔH]	Ch	T_{tr} [ΔH]	BP	T_{tr}
5ZBL	77 [+17.5]	75 [−10.8]	—		—		•	153 [−0.02]	•	160 [−0.48]	•	190 [−0.65]	—	
7ZBL	66 [+22.4]	44 [−27.3]	—		—		•	160 *	•	166 [−0.40]	•	182 [−0.21]	—	
8ZBL	43 [+10.3]	24 [−7.4]	—		—		•	162 [−0.01]	•	163 [−0.35]	•	180 [−0.64]	•	181 *
9ZBL	47 [+13.6]	31 [−12.0]	•	58 *	•	96 [−0.02]	•	158 [−0.01]	•	160 [−0.41]	•	174 [−0.27]	•	175 *
10ZBL	63 [+20.1]	35 [−12.9]	—		•	115 *	•	160 [−0.01]	•	163 [−0.57]	•	173 [−0.66]	•	175 *

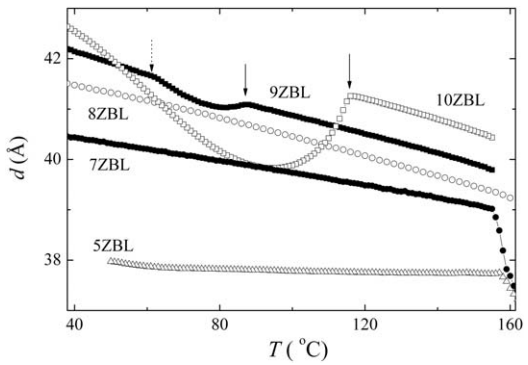

Fig. 3 Temperature dependencies of the layer spacing taken on cooling for denoted compounds. For **9ZBL** and **10ZBL** arrow indicates the SmA*-SmC* phase transition, for **9ZBL** the dotted arrow marks the SmC*-SmA^*_{RE} phase transition.

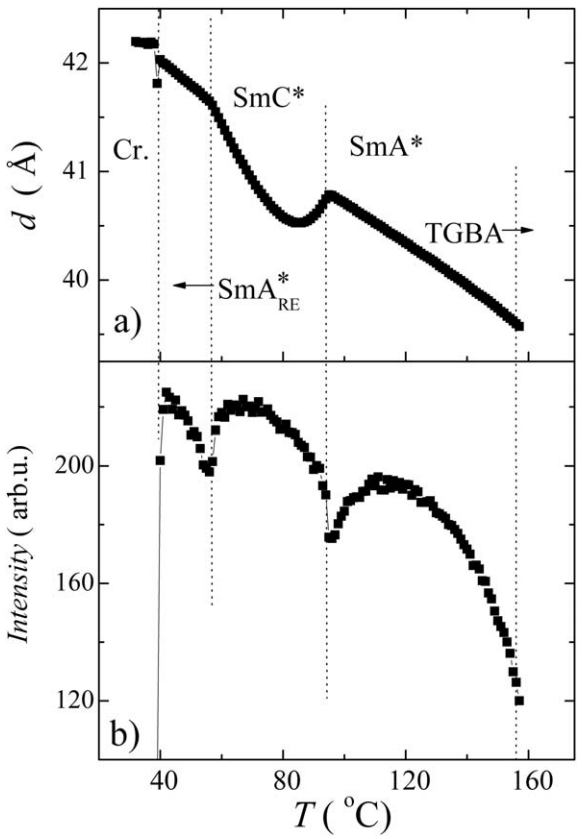

Fig. 4 Temperature dependencies of the layer spacing, d, and intensity of X-ray peak for **9ZBL**. Phases are denoted, dotted lines mark phase transition temperatures.

of the dielectric strength, $\Delta\varepsilon$, and relaxation frequency, f_r, have been established. For **9ZBL** temperature dependencies of both quantities are shown in Fig. 5. One can see a linear decrease of relaxation frequency of the soft mode observed in the SmA* phase above the SmA*-SmC* phase transition (Fig. 5a). In the SmC* phase a Goldstone mode (collective azimuthal director fluctuations) overwhelmed the soft mode contribution and $\Delta\varepsilon$ reaches rather high values, a maximum of about 30 has been found for **9ZBL** and about 50 for **10ZBL**. In contrast to **10ZBL** with increasing $\Delta\varepsilon$ on cooling within the whole temperature range of the SmC* phase, for **9ZBL** $\Delta\varepsilon$ starts to decrease when approaching the SmC*-SmA^*_{RE} phase transition. At the SmC*-SmA^*_{RE} phase transition a steep decrease of $\Delta\varepsilon$ and a minimum of f_r occurs (see inset of Fig. 5a). For **10ZBL** a continuous decrease of $f_r(T)$ has been found on cooling within the SmC* phase (empty points in the inset of Fig. 5a). Such a decrease of f_r is typical and is usually connected with an obvious increase of rotational viscosity of the Goldstone mode with decreasing temperature.

We have also performed permittivity measurements under a bias field. Under the bias field the Goldstone mode in the SmC* phase is suppressed. In Fig. 6, a 3D graph of the imaginary part of dielectric permittivity under bias 3 V μm^{-1} is presented for **9ZBL**. Two distinct anomalies corresponding to the SmA*-SmC* and SmC*-SmA^*_{RE} phase transitions are present. Temperature dependences of f_r and $\Delta\varepsilon$ without bias and under the bias of 1/μm and 3V μm^{-1} are shown in Fig. 7 for **9ZBL**. Suppression of the Goldstone mode is evidenced by a decrease of $\Delta\varepsilon$ with bias and thus a critical dependence of the soft mode could be seen. We have detected a shift of the phase transition temperatures bringing about significant enlargement of the SmC* phase. For **10ZBL** a 3D graph of the imaginary part of permittivity under bias 3 V μm^{-1} is presented in Fig. 8. Additionally to the SmA*-SmC* peak at 117 °C a very small anomaly appeared at about 68 °C. Temperature dependencies of fitted values of $\Delta\varepsilon$ and f_r under bias 3 V μm^{-1} are shown in Fig. 9 for **10ZBL**. The soft mode is clearly visible at the SmA*-SmC* transition. A slight anomaly at 68 °C might indicate pre-transitional effects of a non-realized SmA^*_{RE} phase.

Spontaneous tilt angle and polarization

Methods for measurement of both quantities, tilt angle as well as polarization, require application of an electric field high enough

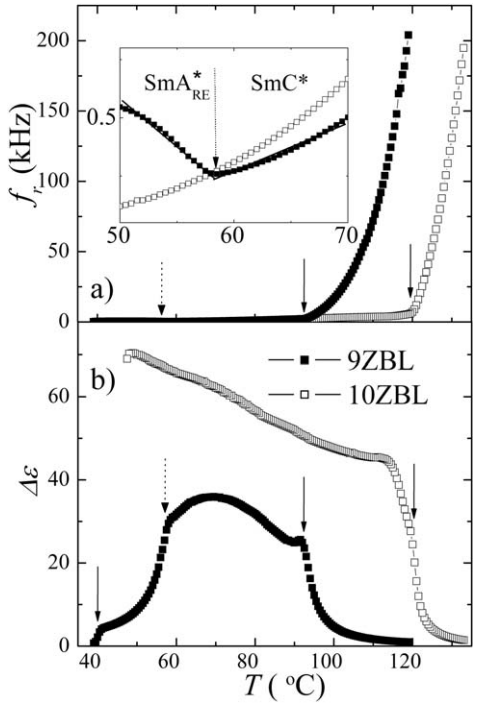

Fig. 5 Temperature dependence of a) the relaxation frequency, f_r, and b) dielectric strength, $\Delta\varepsilon$, for **9ZBL** (full symbols) and **10ZBL** (empty symbols). The inset shows temperature dependence of f_r in enlarged view in the vicinity of the SmC*-SmA*$_{RE}$ phase transition. Arrows mark phase transitions. The first arrow from left side is for crystallization and dotted arrows are for the SmC*-SmA*$_{RE}$ phase transition.

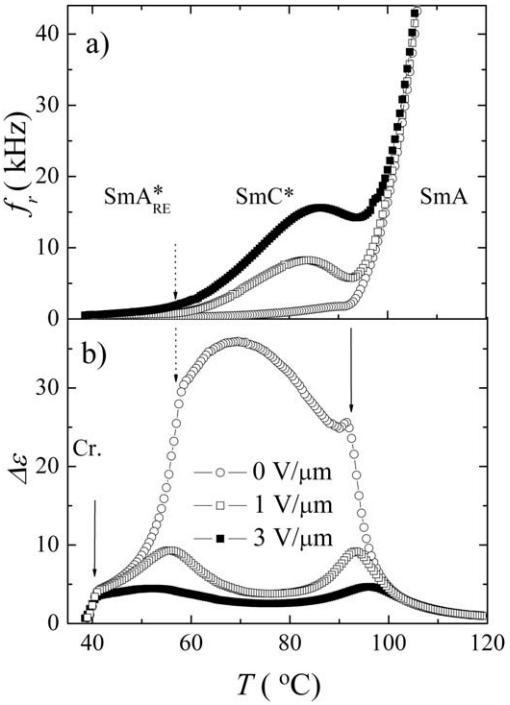

Fig. 7 Temperature dependencies of the relaxation frequency, f_r, and the dielectric strength, $\Delta\varepsilon$, for **9ZBL** without field and under the indicated bias field. Empty circles are for measurement without field, empty squares for 1 V μm^{-1} and full symbols for 3 V μm^{-1}. Arrows show phase transition temperatures for zero bias field.

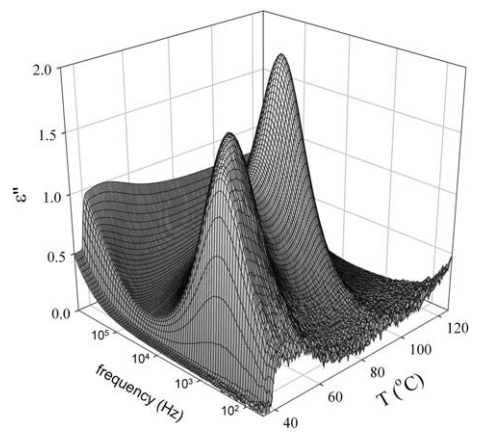

Fig. 6 Three-dimensional graph of the imaginary part of the dielectric permittivity *versus* temperature and frequency for **9ZBL** measured in bias of 3 V μm^{-1}.

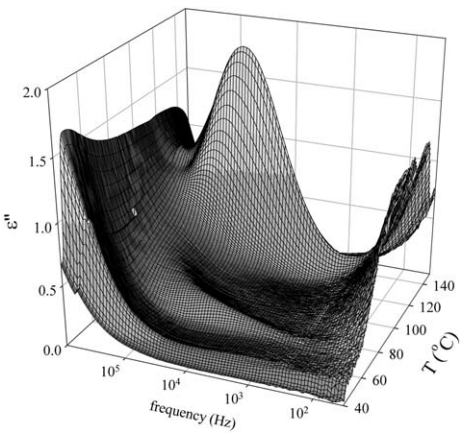

Fig. 8 Three-dimensional graph of the imaginary part of the dielectric permittivity *versus* temperature and frequency for **10ZBL** measured in bias of 3 V μm^{-1}.

for ferroelectric switching, so that zero field values are not accessible. Typically, in ordinary SmC* phases the measured values are not significantly affected by measuring in a field higher than the switching threshold with the exception of when in close vicinity of the SmA*-SmC* phase transition. In the case of **9ZBL** with a quite unique phase sequence, the measuring field influences the values of both tilt angle and polarization within the whole range of the SmC* phase. Besides, the upper and lower temperature limits of the SmC* phase are shifted under the field extending the width of this phase (see also the dielectric properties). Out of the limits of the SmC* phase only an electroclinic effect takes place. For **9ZBL** the tilt angle, θ, increases continuously with the field up to 15 V μm^{-1}, where saturation occurs[4] (see Fig. 10a for low bias field). From dielectric spectroscopy data (Fig. 7) we can estimate the temperatures for both SmA*-SmC* and SmC*-SmA*$_{RE}$ phase transitions under fields of up to 3 V μm^{-1}, taking them as maxima in $\Delta\varepsilon(T)$ dependence, and for higher bias fields the transition temperatures are linearly extrapolated. In Fig. 10a dotted lines mark the phase transition

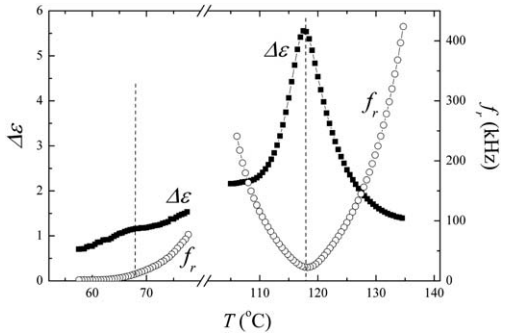

Fig. 9 For **10ZBL** temperature dependencies of dielectric strength, $\Delta\varepsilon$, in full symbols and of the relaxation frequency, f_r, in empty symbols measured under bias field of 3 V μm^{-1}.

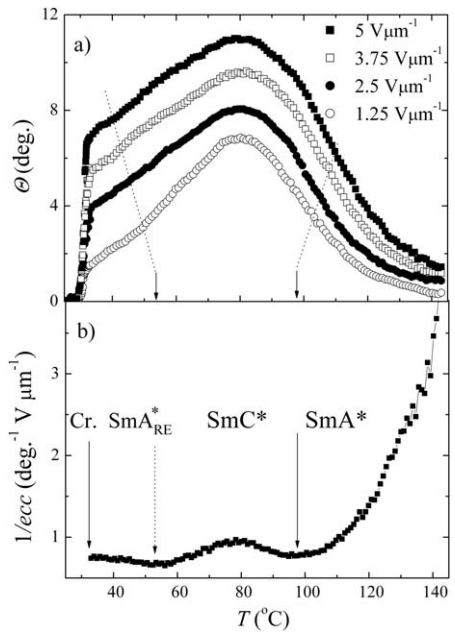

Fig. 10 Temperature dependencies of a) tilt for indicated measuring field and b) reciprocal electroclinic coefficient, 1/*ecc*, calculated as a slope of the tilt angle field dependence (upper dependencies) for **9ZBL**.

temperatures taken from the dielectric data. The values of θ within the SmC* phase comprise both spontaneous tilt and the induced tilt under the field, the later is known as an electroclinic effect.[8]

For **9ZBL** the electroclinic effect contribution is extremely high, offering angles comparable with the spontaneous tilt. Up to the bias field of about 5 V μm^{-1} the tilt angle dependence on the applied field is practically linear and the slope of the tilt *versus* electric field gives values of the electroclinic coefficient, *ecc*. Rather high values of *ecc* have been obtained for **9ZBL** reaching a maxima up to 2 deg V^{-1} μm at the SmA*-SmC* and SmC*-SmA*$_{RE}$ phase transitions. Temperature dependence of the reciprocal value of *ecc* (1/*ecc*) for **9ZBL** is presented in Fig. 10b. One can see the softening of 1/*ecc*(T) at the SmA*-SmC* and SmC*-SmA*$_{RE}$ phase transitions. Similarly to the temperature dependence of dielectric strength and relaxation frequency measured by dielectric spectroscopy, *ecc* evidences that on approaching the tilted–non-tilted phase transition the collective fluctuations slow down and finally freeze to form the ferroelectric phase.[9]

The tilt of molecules, θ_x, can be also estimated from the layer spacing temperature dependence using a formula $\cos\theta_x = d_{SmC}/d_{SmA^*}$ from the layer spacing measured in the SmC* phase, d_{SmC}, and the linearly extrapolated value of $d(T)$ from the SmA* phase, d_{SmA^*}. The layer spacing data are obtained in zero electric field. Let us compare values of θ_x with the tilt measured electro-optically under low electric field (Fig. 10a). The comparison shown in Fig. 11a exhibits qualitatively similar temperature behaviour, only the data measured under the electric field are higher due to the electroclinic effect. The departure of both curves is gradually stronger when approaching the phase transitions to both SmA* phases because of the increasing electroclinic effect and also due to the shift of the transition temperatures under the electric field.

For **10ZBL** the temperature dependencies of both tilt angle values determined optically and from the layer spacing data are shown in Fig. 11b. Both curves exhibit a significant decrease on cooling within about 50 K. Such dependence is quite unusual in the SmC* phases, where saturation of the tilt angle value typically occurs on decreasing temperature. One can expect that the

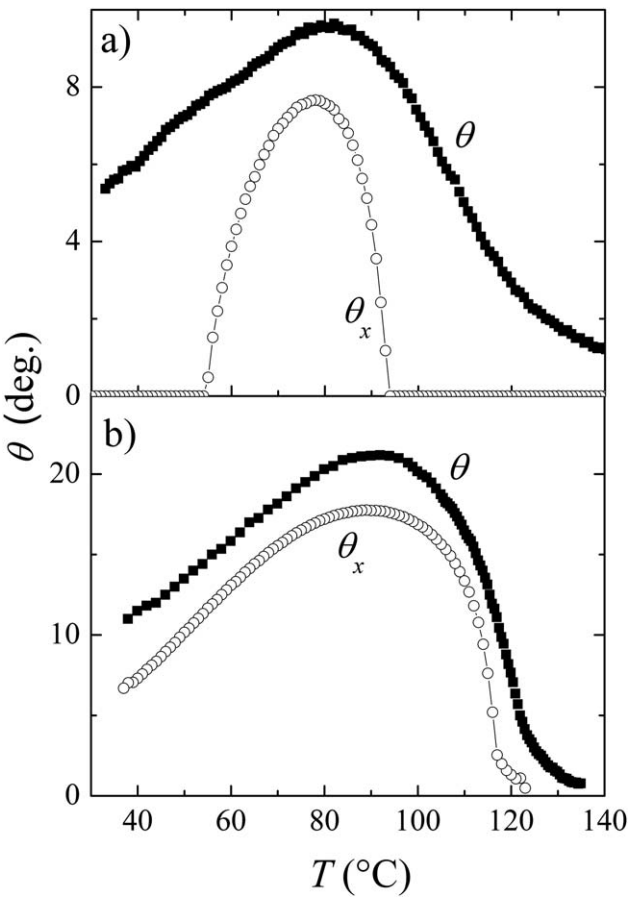

Fig. 11 Temperature dependencies of the tilt angle, θ, measured electro-optically in electric field $E = 4$ V μm^{-1} are compared with the tilt angle detected from the layer spacing data (empty symbols) using the relationship $\cos\theta = d_{SmC}/d_{SmA^*}$ between the layer spacing measured in the SmC* phase, d_{SmC}, and the linearly extrapolated value from the SmA* phase, d_{SmA^*}, for a) **9ZBL** and b) **10ZBL**.

behaviour found here is based on the same mechanism as the appearance of the SmA^*_{RE} phase in the next homologue **9ZBL**.

The spontaneous polarization has been measured for both **9ZBL** and **10ZBL** (Fig. 12). For **9ZBL** the temperature range of the SmC* phase is significantly widened under the field, similarly as it is observed in the optical measurement of the tilt angle. The techniques of polarization measurements by means of integration of the switching current or from the hysteresis loop allow to eliminate the field induced linear effect (permittivity), so that the measured values of P include the spontaneous polarization and non-linear induced polarization only. When approaching the limits of the SmC* phase the hysteresis loop becomes thinner as the threshold field for switching is decreasing. Out of the limits of the SmC* phase the loop becomes theoretically infinitely thin, representing only non-linear polarization. In reality, behind the zero-field limits of the SmC* phase the width of the loop might be finite because of the graduate shift of the phase transition under increasing field during switching. Due to this effect the non-linear induced polarization cannot be completely distinguished from the spontaneous polarization. For both **9ZBL** and **10ZBL** temperature dependence of the spontaneous polarization shows continuous decrease on cooling after reaching a maximum at about 90 °C. In literature such an anomalous decrease of $P(T)$ on cooling within the SmC* phase is connected with inversion of the spontaneous polarization sign.[10] In the case of both studied compounds the behaviour of $P(T)$ is most probably connected with the same mechanism as the decrease of the tilt angle.

Both compounds differ in the value of saturation field, above which the polarization and the tilt angle do not increase. For **9ZBL** it is 15 V μm^{-1}, while for **10ZBL** it is only 5 V μm^{-1}.

Discussion and conclusions

We have prepared and studied a homologue series of compounds exhibiting rather strong chirality, which is manifested by occurrence of TGB and/or blue phases. High chirality is related to the presence of two chiral centres in the terminal chiral chain. For all homologues the SmA* phase occurs. Compounds with longer non-chiral chain **9ZBL** and **10ZBL** exhibit the ferroelectric SmC* phase. For homologue **9ZBL** another smectic A phase occurs below the ferroelectric SmC* phase. We assigned this phase to a re-entrant smectic A phase, SmA^*_{RE}, and it is the first example of paraelectric re-entrant smectic A phase below the SmC* phase. The SmA^*_{RE} phase has very similar structural parameters as the upper SmA* phase, which is a difference from previously studied re-entrancy of smectic A phase in non-chiral compounds, where dimerization is responsible for the re-entrancy.[1]

For **9ZBL** the layer spacing data, d, established in the SmA^*_{RE} phase follows a nearly linear continuation of the temperature dependence of d in the upper SmA* phase (see Fig. 3). This fact suggests that both phases are built from the same objects, just simple molecules. The reason for the increase of d on cooling in the SmA* phase is probably the increase of the orientational order and gradual extension of terminal chains. The same ordering effect might be behind the temperature dependence of d found for **10ZBL**, where on cooling, after the decrease of d due to tilt of molecules, values of d reach the extrapolated line from the temperature dependence in the SmA* phase. In the temperature dependencies of the layer spacing, $d(T)$, presented in Fig. 3 we can see that the higher the terminal chain length (higher n value), the higher the thermal expansion coefficient value (higher slope of $d(T)$ dependence). It indicates that the chains play an active role in bringing about the re-entrancy.

One can expect that both effects described above, namely the increase of the orientational order and extension of the terminal chains become gradually saturated on decreasing temperature and another mechanism may become active. We propose a model with sterical hindrance in packing of the molecules within the smectic layers because of the bulky chlorine atom laterally substituted in the molecular core as it is shown in Fig. 13. In the SmC* phase, at first, layer spacing falls down due to the tilt of molecules (*cf.* Fig. 13a, b). Simultaneously, density as well as quadrupolar ordering increases on cooling, which may result in a shift of molecule mass centres due to the hindrance effect of the chlorine atom (*cf.* Fig. 13b, 13c, 13d). Such a mechanism can explain the slightly higher thermal expansion coefficient in the SmA^*_{RE} phase compared to that in the SmA* phase. It can also clarify the discrepancy between the molecular length calculated using ChemOffice in a range of 40–41 Å for fully extended terminal chains, and a slightly higher layer spacing detected in the orthogonal SmA^*_{RE} phase. (*cf.* Fig. 13a, 13d).

For compound **10ZBL** a regular phase sequence SmA*-SmC* occurs; nevertheless specific anomalies have been observed within the SmC* phase. It is a significant decrease of the tilt and polarization values on cooling and a small anomaly in dielectric data when the Goldstone mode is suppressed by a bias electric field. It allows us to consider that homologue **10ZBL** reveals similar tendencies that bring about the paraelectric SmA^*_{RE} phase in **9ZBL**. From a phenomenological point of view the re-entrancy in **9ZBL** was explained by non-monotonous temperature dependence of the lowest term coefficient in the expansion of

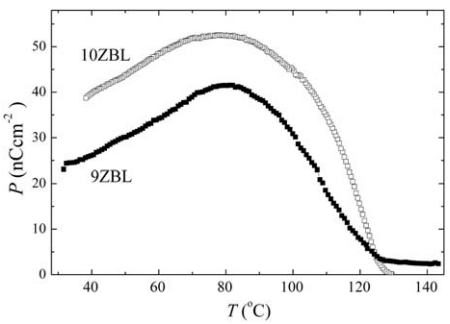

Fig. 12 Temperature dependencies of polarization measured at electric field of 15 V μm^{-1} for **9ZBL** (full symbols) and **10ZBL** (empty symbols).

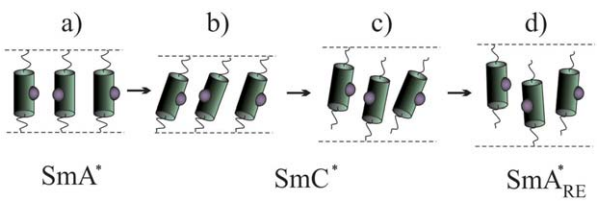

Fig. 13 Model for the molecular arrangement in the layer for the phase sequence SmA*-SmC*-SmA^*_{RE}.

the free energy with the tilt angle as a transition parameter.[4] It was supposed that this term changes sign twice, at the SmA*-SmC* and SmC*-SmA*$_{RE}$ phase transitions. Along this line, we consider that in **10ZBL** the value of the lowest term just approaches zero without reaching full softening and transition to the SmA*$_{RE}$ phase.

We can find several similarities in molecular properties of studied ferroelectric homologues **9ZBL** and **10ZBL** and compounds exhibiting inversion of polarization and/or tilt angle.[10] Contrary to obvious temperature dependencies in the SmC* phase, values of polarization and tilt fall down. For compounds with inversion these quantities change their sign at an inversion temperature and we can imagine that at this temperature the SmA* structure occurs. This rare anomaly has been observed for fluorine-laterally substituted terphenyl derivatives with two chiral centers.[10a] We can expect that the presence of multiple chiral centers is important also in our case. Styring *et al.*[10a] explained the inversion effect taking into account competition of various molecular conformations. We suppose that in **9ZBL**, due to a similar mechanism the SmA*$_{RE}$ phase appears on cooling after the SmC* phase and then persists within a certain temperature interval till crystallization.

Generally, for anomalous phase behaviour occurrence of multiple chiral centres may be important as well as various conformations with respect to the chiral chain and their concentrations change with temperature. Lots of effects such as dipolar interactions, packing arrangements, rotational distribution of various conformers play a significant role in the phase stability.

For conclusion let us mention that the ferroelectric compound with the SmA*$_{RE}$ phase represents a new chance for technical applications. The SmA*$_{RE}$ phase is very sensitive to an electric field which can easily extend the SmC* phase to lower temperatures at the expense of the SmA*$_{RE}$ phase. Strong electroclinic effect was found not only near the SmA*-SmC* phase transition, which is typical, but within a wide temperature interval of the SmA*, SmC* and SmA*$_{RE}$ phases. These properties are promising for electrooptic applications especially when grey-scale capability and fast response is required.

Acknowledgements

This work is supported by grant P204/11/0723 from the Grant Agency of the Czech Republic and by projects IAA100100911 (Grant Agency of ASCR) and SVV-2011-263303. The X-ray diffraction measurements were performed at the Structural Research Laboratory, Chemistry Department, University of Warsaw, Poland, which has been established with financial support from European Regional Development Fund, project No: WKP 1/1.4.3./1/2004/72/72/165/2005/U.

Notes and references

1 (*a*) P. E. Cladis, *Physical Properties of Liquid Crystals*, ed. D. Demus, J. Goodby, G. W. Gray, H.-W. Spiess, V. Vill, Wiley-VCH, 1999, p. 288–303; (*b*) P. E. Cladis, R. K. Bogardus and D. Aadsen, *Phys. Rev. A: At., Mol., Opt. Phys.*, 1978, **18**, 2292–2306; (*c*) S. Singh, *Phase Transitions*, 2000, **72**, 183–200; (*d*) P. E. Cladis, *Phys. Rev. Lett.*, 1975, **35**, 48–51; (*e*) F. Harduin and A. M. Levelut, *J. Phys.*, 1980, **41**, 41–46; (*f*) V. N. Raja, R. Shasidar, B. R. Ratna, G. Hepke and Ch. Bahr, *Phys. Rev. A: At., Mol., Opt. Phys.*, 1988, **37**, 303–305; (*g*) Ch. Y. Yelamaggat, I. S. Shashikala, D. S. Shankar Rao, G. G. Nair and S. Krishna Prasad, *J. Mater. Chem.*, 2006, **16**, 4099–4102; (*h*) S. Abraham, V. A. Mallia, K. V. Ratheesh, N. Tamaoki and S. Das, *J. Am. Chem. Soc.*, 2006, **128**, 7692–7698.

2 (*a*) U. Pietrasik, J. Szydłowska, A. Krówczyński, D. Pociecha, E. Górecka and D. Guillon, *J. Am. Chem. Soc.*, 2002, **124**(30), 8884–8890; (*b*) D. Pociecha, E. Gorecka, M. Čepič, N. Vaupotič, B. Žekš, D. Kardas and J. Mieczkowski, *Phys. Rev. Lett.*, 2000, **86**, 3048–3051; (*c*) V. Novotná, M. Glogarová, V. Hamplová and M. Kašpar, *J. Chem. Phys.*, 2001, **115**, 9036–9041; (*d*) D. S. Shankar Rao, S. Krishna Prasad, V. N. Raja, C. V. Yelamaggad and S. Anitha Nagamani, *Phys. Rev. Lett.*, 2001, **87**, 085504-1–4; (*e*) C. V. Yelamaggad, V. Tamilenthi, D. S. Shankar Rao, G. G. Nair and S. Krishna Prasad, *J. Mater. Chem.*, 2009, **19**, 2906–2908.

3 (*a*) S. L. Wu and C. Y. Lin, *Liq. Cryst.*, 2004, **31**, 1613–1617; (*b*) S. L. Wu and C. Y. Lin, *Liq. Cryst.*, 2005, **32**, 1243–1249; (*c*) E. Dzik, J. Mieczkowski, E. Gorecka and D. Pociecha, *J. Mater. Chem.*, 2005, **15**, 1255–1262; (*d*) S.-L. Wu and H.-N. Hsu, *Liq. Cryst.*, 2007, **34**, 1159–1165; (*e*) V. Novotná, M. Kašpar, V. Hamplová, M. Glogarová, I. Rychetský and D. Pociecha, *Liq. Cryst.*, 2004, **31**, 1131–1141; (*f*) A. Bubnov, V. Hamplová, M. Kašpar, M. Glogarová and P. Vaněk, *Ferroelectrics*, 2000, **243**, 27–35; (*g*) A. Bubnov, V. Novotná, V. Hamplová, M. Kašpar and M. Glogarová, *J. Mol. Struct.*, 2008, **892**, 151–157.

4 V. Novotná, M. Glogarová, M. Kašpar, V. Hamplová, E. Gorecka, D. Pociecha and M. Cepic, *Phys. Rev. E: Stat., Nonlinear, Soft Matter Phys.*, 2011, **83**, 020701(R).

5 A. Langhoff and F. Giesselmann, *ChemPhysChem*, 2002, **3**, 424–432.

6 (*a*) H.-S. Kitzerow, H. Schmid, A. Ranft, G. Heppke, R. A. M. Hikmet and J. Lub, *Liq. Cryst.*, 1993, **14**, 911–916; (*b*) H.-S. Kitzerow, P. P. Crooker, S. L. Kwok, J. Xu and G. Heppke, *Phys. Rev. A: At., Mol., Opt. Phys.*, 1990, **42**, 3442–3448; (*c*) J. Rokunohe and A. Yoshizawa, *J. Mater. Chem.*, 2005, **15**, 275–279; (*d*) S. Meiboom and M. Sammon, *Phys. Rev. Lett.*, 1980, **44**, 882–885.

7 A. Dierking, *Textures of Liquid Crystals*, WILEY-VCH Verlag GmbH, 2003.

8 (*a*) J. V. Selinger, P. J. Colins and R. Shashidhar, *Phys. Rev. E: Stat. Phys., Plasmas, Fluids, Relat. Interdiscip. Top.*, 2001, **64**, 061705 1–9; (*b*) M. S. Spector, P. A. Heiney, J. Naciri, B. T. Weslowski, D. B. Holt and R. Shashidhar, *Phys. Rev. E: Stat. Phys., Plasmas, Fluids, Relat. Interdiscip. Top.*, 2000, **61**, 1579–1584; (*c*) N. Kapernaum, D. M. Walba, E. Korblova, C. Zhu, C. Jones, Y. Shen, N. A. Clark and F. Giesselmann, *ChemPhysChem*, 2009, **10**, 890–892.

9 M. Glogarová, Ch. Destrade, J. P. Marcerou, J. J. Bonvent and H. T. Nguyen, *Ferroelectrics*, 1991, **121**, 285–294.

10 (*a*) P. Styring, J. D. Vuijk, I. Nishiyama, A. J. Slaney and J. W. Goodby, *J. Mater. Chem.*, 1993, **3**(4), 399–405; (*b*) K. Yoshino, H. Taniguchi and M. Ozaki, *Ferroelectrics*, 1989, **91**, 267–276; (*c*) K. Nakao, M. Ozaki and K. Yoshino, *Japanese Journal of Appl. Physics*, 1987, **26–2**, 104–106.

